# Numerical Analyses of the Molecular Dynamics in the Mass Ratio—Energy Plane for the Classical Morse System with Two Degrees of Freedom

Akira NARITA

The periodic orbits and the fixed points in the surfaces of section are analyzed numerically in the mass ratio-energy plane for the Morse system with two degrees of freedom. They are survivals of those in the harmonic limit and can be identified by the same rational rotation numbers as in this limit, and the presence regions of them spread with mass ratio in increasing energy. These results can explain the mass ratio dependence of bifurcation patterns showed by Matsushita and Terasaka, and are very closely connected with the KAM theorem.

## I. Introduction

The molecular dynamics in the linear symmetrical triatomic molecules of $CX_2$ type such as $CO_2$ has been studied thus far by many authors[1—6]. The sum of two Morse potentials, one for each C—X bond, has been assumed as the total potential energy. The Hamiltonian describing the intramolecular vibrations of this $CX_2$ type molecule is given by the equations[3],

$$H = K + V, \qquad \cdots\cdots\cdots\cdots\cdots\cdots\cdots\cdots\cdots\cdots\cdots\cdots\cdots\cdots\cdots\cdots\cdots\cdots\cdots\cdots\cdots\cdots(1)$$

$$K = \frac{m_1(m_1 + m_2)}{2m_1 + m_2} \left[\frac{1}{2}(\dot{r}_1^2 + \dot{r}_2^2) + \gamma \dot{r}_1 \dot{r}_2\right], \qquad \cdots\cdots\cdots\cdots\cdots\cdots\cdots\cdots\cdots\cdots(2)$$

$$V = D[1 - \exp(-ar_1)]^2 + D[1 - \exp(-ar_2)]^2, \qquad \cdots\cdots\cdots\cdots\cdots\cdots\cdots\cdots(3)$$

$$\gamma = \frac{m_1}{m_1 + m_2} \, (0 < \gamma < 1), \qquad \cdots\cdots\cdots\cdots\cdots\cdots\cdots\cdots\cdots\cdots\cdots\cdots(4)$$

where K=(internal kinetic energy), V=(total potential energy), $m_1$=(mass of X—atom), $m_2$=(mass of C—atom), $r_i$=(displacement from the equilibrium bond distance), a=(scale parameter), D=(dissociation energy of C—X bond) and $\dot{r}_i = dr_i/dt$ (t : time). This model has two parameters, mass ratio dependent parameter $\gamma$ and energy E. The $\gamma$ values for some molecules are as follows, $\gamma=0.4673$ for $N_2O$, $\gamma=0.5714$ for $CO_2$, $\gamma=0.5968$ for $BO_2$ and $\gamma=0.7273$ for $CS_2$.

More recently, for this model system, Matsushita and Terasaka [2] showed the pattern changes in Poincaré surfaces of section as a function of $\gamma$, due to bifurcations of various fixed points from the central island [18]. Furthermore, they plotted the relative area of the central islands to the whole region as functions of $\gamma$ assuming that the region except the central islands are chaotic. The plots showed that the $\gamma$-dependence of the area is oscillating. These are very interesting results. Particularly, the area is almost zero at $\gamma=0.263$ for E=D because of the 3:1 resonance [7]. At this $\gamma$, the 3—fixed points degenerate to the central 1—fixed point. From this situation, the almost complete ergodic behaviour can be seen at $\gamma=0.263$.

My main purpose is to clarify the origin of the pattern changes in the Poincaré surfaces of section mentioned above. I will proceed by considering the modifications of the periodic orbits in the harmonic

Numerical Analyses of the Molecular Dynamics in the Mass Ratio–Energy
Plane for the Classical Morse System with Two Degrees of Freedom
— 111 —

limit for E→0, due to the nonlinear effect of the present Morse potential. The calculations will be carried out numerically based on the model given by eqs. (1)–(4), as will be described in the following sections.

## 2. Equations of motion

In eqs. (2)–(3), introducing the dimensionless variables, $x = a(r_1 + r_2)$, $y = a(r_1 - r_2)$ and $\tau = a[2D(2m_1 + m_2)/m_1(m_1 + m_2)]^{1/2}t$, we can get the equations,

$$K = \frac{1}{2(1+\gamma)} p_x^2 + \frac{1}{2(1-\gamma)} p_y^2, \quad \dots\dots\dots\dots(5)$$

$$V = 2 - 4\exp(-x/2)\cosh(y/2) + 2\exp(-x)\cosh(y), \quad \dots\dots\dots(6)$$

where $p_x$ and $p_y$ are momentums conjugate to $x$ and $y$, respetively, and D is adopted as energy unit (D=1). The equations of motion can be easily derived from eqs. (5) and (6),

$$\dot{x} = p_x/(1+\gamma), \quad \dot{y} = p_y/(1-\gamma), \quad \dots\dots\dots\dots(7)$$

$$\dot{p}_x = -2\exp(-x/2)\cosh(y/2) + 2\exp(-x)\cosh(y), \quad \dots\dots\dots(8)$$

$$\dot{p}_y = 2\exp(-x/2)\sinh(y/2) - 2\exp(-x)\sinh(y), \quad \dots\dots\dots(9)$$

where $\cdot = \frac{d}{d\tau}$. This system is separable for $\gamma = 0$, as easily seen from eqs. (2) and (3) [2]. The solution for $\gamma = 0$ is given by the equation,

$$r_i = a^{-1}\ln[A_i + B_i\cos(\omega_i\tau + \phi_i)], \quad [B_i^2 = A_i(A_i - 1), \quad \omega_i^2 = A_i^{-1}]. \quad \dots\dots\dots(10)$$

where $A_i$ and $\phi_i$ are integral constants. This system is also separable for $\gamma = 1$[2]. We get $p_y \equiv 0$ for $\gamma = 1$. This leads to $y = 0$ or $\exp(-x/2)\cosh(y/2) = 1/2$ from eq. (9). The former gives the Thiele–Wilson solution [3], and the latter gives the solution,

$$\exp(x) = \frac{1}{2\omega^2} \times \begin{cases} \sin^2(\omega\tau + \phi) \ [\omega = (1-E)^{1/2}/2 \text{ for } E<1] \\ \sinh^2(\omega\tau + \phi) \ [\omega = (E-1)^{1/2}/2 \text{ for } E>1]. \end{cases} \quad \dots\dots\dots(11)$$

The present system can not be separable for $0 < \gamma < 1$[2].

The second and the third order terms of the present Morse potential V agrees with the harmonic and the anti–Hénon–Heiles type potentials [8], respectively. In the harmonic limit, $\omega_1 = (1+\gamma)^{-1/2}$ and $\omega_2 = (1-\gamma)^{-1/2}$ are frequencies. The rotation number $\alpha$[9] in this limit is given by the equation,

$$\alpha = \omega_1/\omega_2 = [(1-\gamma)/(1+\gamma)]^{1/2} \ (0<\alpha<1). \quad \dots\dots\dots(12)$$

The equations of motion given by eqs. (7)–(9) were numerically integrated by means of the RKG method. The accuracies in numerical calculations were checked by comparing the energy given at the first step of iteration with that obtained at the last step of it. Errors in both energies were less than 0.5%. All initial values were taken on the equipotential surface, since the Poincaré surfaces of section ($y = 0$ and $p_y > 0$) can be completely filled with traverses of the phase curves obtained by moving them along it. The numerical results obtained in this way will be described in later sections.

## 3. Periodic orbits

The trajectories in the harmonic system are defined by the equation $x = A_1\cos\alpha\tau$ and $y = A_2\cos(\tau + \phi)$, where $A_i$ and $\phi$ are integral constants. Note that $\alpha$ is defined by eq. (12) and $\phi$ is the phase difference. The trajectory identified by $\alpha$ and $\phi$ will be represented by $H(\alpha, \phi)$ below. The properties of $H(\alpha, \phi)$ are well known[10], and they have been referred to as the Lissajous figures.

Since the second order term in the pre-
sent Morse potential agrees with the har-
monic potential, my interests concentrate on
the modifications of H($\alpha$, $\phi$) due to the non-
linear effect of the potential, particularly for
the rational rotation number $\alpha = m/n$.

The periodic orbits obtained numerically
for the present Morse system are shown in
fig. 1 for some rational $\alpha$. In fig. 1, E=0.4 is
selected and $\gamma$ values are calculated from eq.
(12) for given $\alpha$. This figure indicates that
the periodic orbits in the harmonic limit can
survive only for the particular phase differ-
ences. That is, only the periodic orbits, cor-
responding to $\phi=0$ for even m and to $\phi=0$
(solid line in fig. 1) and $\pi/m$ (dashed line) for
odd m, can survive. However, it should be
noted that these periodic orbits are distorted
from those in the harmonic system because
of the nonlinear effect of the Morse potential.
Only particular initial value can give the
periodic orbits shown in fig. 1. However, the
problem obtainig the initial value for the
periodic orbit identified by $\alpha$ and $\phi$ is not
referred here. These periodic orbits are sta-
ble concerning the slight shift of the initial
value. Then they become fat and change
into the periodic tube[11]. In fact, these give
the elliptic fixed points in the x-$p_x$ Poincaré
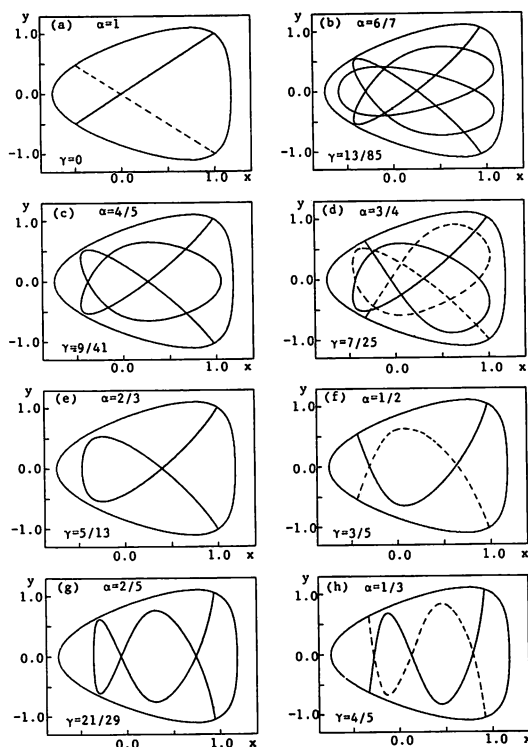surfaces of section, and the periodic tubes



Fig. 1 Survivals of the periodic orbits in the harmonic
limit for some rational rotation numbers $\alpha=m/n$. $\alpha$ is re-
lated to $\gamma$ by eq. (12). The most outer boundary in each
figure is the equipotential curve for E=0.4. For odd m,
the solid and the dashed lines show the periodic orbits
identified by $\phi=0$ and $\phi=\pi/m$, respectively.

give the islands of the fixed points[1]. The survived periodic orbit characterized by rational $\alpha(=m/n)$ with
even m gives the n-elliptic fixed points, as easily seen from fig. 1. For odd m, because there are two stably
survived periodic orbits corresponding to $\phi=0$ and $\pi/m$, and each of them gives the n-elliptic fixed points,
they totaly give the 2n-elliptic fixed points. Note that $\alpha$ is the average rotation number.

The numerical calculations furthermore clarified that H(m/n, $\pi/m$) for even m and H(m/n, $\pi/2m$) for
odd m can survive. However, because they are unstable concerning the slight change of the initial value,
they give the k−hyperbolic fixed points (k=n for even m and k=2n for odd m) in the x−$p_x$ surfaces of
section. It should be emphasized that the 3 : 1 resonance can be understood as transition of the phase
difference for the periodic orbit identified by $\alpha=2/3$ from $\phi=0$ to $\phi=\pi/2$, due to the instability of the
orbit[2]. It should be noted that the periodic orbit corresponding to $A_1=0$ and $A_2 \neq 0$ in the harmonic
system can also survive. This orbit is stable concerning the slight change of the initial value and gives the
central 1−fixed point[1, 2]. The periodic orbit corresponding to $A_1 \neq 0$ and $A_2=0$ can also exist, while
unstable concerning the initial value, and gives the boundary in the x−$p_x$ surfaces of section. This will be
referred to as the Thiele−Wilson mode[1−3].

The reason that E=0.4 is chosen in fig. 1 is that this energy is convienient for serching the survivals
of H(m/n, $\phi$) because of no visually chaotic motions. We reported for $CO_2$ molecule that visually chaotic

Numerical Analyses of the Molecular Dynamics in the Mass Ratio–Energy
Plane for the Classical Morse System with Two Degrees of Freedom

— 113 —

Fig. 2 Presence regions of the representative periodic orbits identified by the rational rotation numbers $\alpha = 1$, 4/5, 2/3, 1/2 and 2/5 in the $\gamma$-E plane. Serching the right boundary in each region numerically is very difficult for E>0.7 with exception of $\alpha = 1$ because of abundant chaotic motions. Then, very small interval of $\gamma$ must be taken ($\Delta\gamma = 10^{-4}$). The predicted right boundary curves are shown by the dashed lines, because existences of the periodic orbits could not be verified there. Note that the islands around each elliptic fixed point become abruptly small by the slight increase of $\gamma$ from the left boundaries for E>0.7. The 3:1 resonance can occur on the dot dashed line. See the text about ●
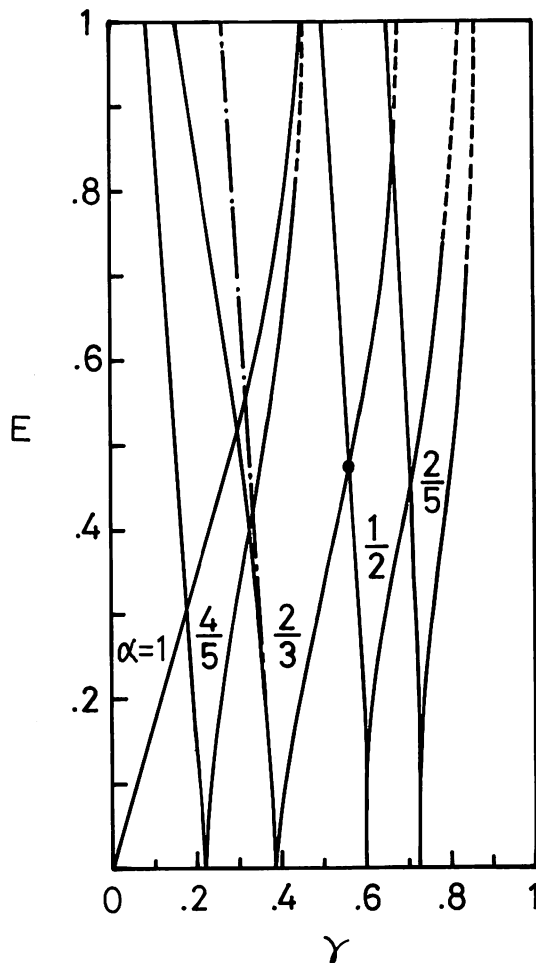


motions can be observed for $E > 0.5$ [1]. According to the numerical calculations performed now, the energy at which chaotic motions begin visually does not almost depends on $\gamma$ except for $\gamma \cong 0$ and $\gamma \cong 1$, and is $E \cong 0.5$. This result is similar to that by Casati and Ford [12]. Note that the chaotic motions are abundant particularly near the boundary in the x-$p_x$ surfaces of section, for E>0.5 [1, 2].

## 4. Separations of the fixed points from the central island

Let us denote $\gamma$ calculated from eq. (12) for $\alpha = m/n$ by $\gamma_{n,m}$. Does the periodic orbit $M(m/n, \phi)$ also exist for slightly shifted $\gamma$ from $\gamma_{n,\lambda}$? $M(m/n, \phi)$ is the periodic orbit in the present Morse system, and it is the survival of $H(m/n, \phi)$, where $\phi = 0$, $\pi/m$ for even m and $\phi = 0$, $\pi/m$, $\pi/2m$ for odd m. Firstly, this question will be solved. Secondly, the origin for the $\gamma$-dependence of the bifurcation showed by Matsushita and Terasaka will be considered.

Numerical calculations showed that $M(m/n, \phi)$ can also exist for slight change of $\gamma$ from $\gamma_{n,m}$. That is, the initial value giving the $M(m/n, \phi)$ can be serched for a range of $\gamma$ including $\gamma_{n,m}$. The presence region of $M(m/n, \phi)$ in the $\gamma$-E plane is shown in fig.2 for some rational rotation numbers. This figure shows that the presence region of $M(m/n, \phi)$ spreads concerning $\gamma$ in increasing E. This figure furthermore shows that $M(m/n, \phi)$ exists until the two body dissociation threshold (E=1), while the islands of each elliptic fixed points become small because of development of chaotic motions in the vicinity of it [1, 2]. In fig.2, the presence region of $M(m/n, \phi)$ are not shown for larger denominators of m/n, because the spread concerning $\gamma$ in increasing energy is small.

Let us increase $\gamma$ for a fixed E. When $\gamma$ crosses the left boundary for the presence region of $M(m/n, \phi)$ in fig.2, an appearence of it begins. Then, in the x-$p_x$ surfaces of section, the k-fixed points with the

Akira NARITA

elliptic or the hyperbolic characters due to M(m/n, $\phi$) (k=n for even m and k=2n for odd m) separate from the central island. On the left boundary curve, M(m/n, $\phi$) is degenerate to the periodic orbit giving the central 1-fixed point. With increasing $\gamma$ from the left boundary, the fixed points due to M(m/n, $\phi$) move toward the boundary in the surfaces of section. When $\gamma$ arrives at the right boundary of M(m/n, $\phi$), the fixed points are on the boundary in the surfaces of section because of degeneracy of M(m/n, $\phi$) to the xaxis (Thiele-Wilson mode).

From the facts mentioned above, the origin for the separations of fixed points concerning $\gamma$ from the central island showed by Matsushita and Terasaka[2] can be now explained more radically. That is, with increasing $\gamma$ for a fixed E, because $\gamma$ goes across the left boundary of M(m/n, $\phi$) in the large order of rational rotation number m/n, the fixed points successively separate from the central island in the same order and move toward the boundary. Note that only the separations of the fixed points identified by the rotation number m/n with small denominator from the central island were given in ref. 2, because the numerical serchings for them with large n are difficult. Since the rational numbers are dense, there can coexist infinitely many chains of fixed points in the surface of section for a point on the $\gamma$–E plane. This may be an explanation for the Poincaré-Birkhoff theorem[13-16] in terms of the survivals and the spreads of the presence region of the periodic orbits in the harmonic limit. For example, for the point indicated by ●in fig.2, the fixed points identified by m/n satisfying $1/2 < m/n < 2/3$ can coexist in the surface of section.

## 5. KAM (Kolmogorov-Arnold-Moser) instabilities

With increasing E for a fixed $\gamma$ in fig. 2, the energy goes across successively the left or the right boundaries of the presence regions for many M(m/n, $\phi$). When the energy crosses each of these boundaries, the resonance conditions can be satisfied. These conditions induce the instabilities for the invariant tori [17]. These tori are giving the central islands and the boundary in the surface of section, immediately before the energy trverses of the left and the right boundaries in fig.2, respectively. The invariant tori are destoried and change into the new tori by the traverses. The new tori give the KAM surfaces around the n-fixed points caused from the M(m/n, $\phi$). The invariant tori can be destoried at smaller E for $\gamma$ near $\gamma_{n,m}$, since then the traverses occur in the smaller E.

Thus, the spreadings of the presence regions for M(m/n, $\phi$) with $\gamma$ in increasing E can be illustration of the KAM theorem itself[13–15]. Therefore, the boundary curves in fig.2 represent a set of points, on which the low order resonances occur. Furthermore, even for the invariant tori identified by the irrational rotation number $\sigma$, it is well known that those with $\sigma$ satisfying the KAM inequality $|\sigma - m/n| < \varepsilon n^{-2.5}$ can be destoried by the perturbation [13–15]. The zone of $\sigma$ determined by the inequality is larger for the smaller n. From this KAM consequence, the fact in fig.2, that the spread of the presence region with $\gamma$ in increasing E is large for M(m/n, $\phi$) with the rotation number of the small denominator, can be also understood qualitatively. I think that the oscillating character concerning $\gamma$ of the relative area of nonchaotic regions[2], described in the section 1, is also related to this large spreading for M(m/n, $\phi$) with the small denominator.

## 6. Discussion

In the Toda system too[19], in which the present Morse potential is replaced by the Toda potential, the similar characteritics as in the present Morse system can be observed for the survivals and the spreads of the periodic orbits in the harmonic limit. But, the chaotic behaviours can not be seen even for the higher energy (at least, E/D=10) because of no dissociation energy. There, the equal coefficient of the second order term was adopted for both potentials. It seems that the conditions, that the potential has the disso-

Numerical Analyses of the Molecular Dynamics in the Mass Ratio−Energy
Plane for the Classical Morse System with Two Degrees of Freedom

— 115 —

ciation energy or the local maximum, may be necessary for the occurrence of chaotic motions[20]. For the system replaced the Morse potential by the Hénon−Heiles potential [21], the movements of the fixed points with increasing $\gamma$ are opposite to those in the present Morse system, and the situation is more complicated, particularly for small $\gamma(0<\gamma<0.2)$. But, Casati−Ford type $E_c$ with $\gamma$ can be also found, except for $\gamma\cong0$ because this system agrees with the original Hénon.−Heiles model for $\gamma=0$[21], where $E_c$ is the energy at which chaotic motions begin to occur. The detailed report on the Toda and the Hénon−Heiles systems will be given in a separate paper.

## Acknowledgment

## References

[1]  T. Matsushita, A. Narita and T. Terasaka, Chem. Phys. Letters **95** (1983) 129.

[2]  T. Matsushita and T. Terasaka, Chem. Phys. Letters **100** (1983) 138.

[3]  E. Thiele and D. J. Wilson, J. Chem. Phys. **35** (1961) 1256.

[4]  C. Jaffé and P. Brumer, J. Chem. Phys. **73** (1980) 5646.

[5]  P. Brumer, Adv. Chem. Phys. **47** (1981) 215, references therein.

[6]  R. T. Lawton and M. S. Child, Mol. Phys. **37** (1977) 1799 ; **40** (1980) 773 ; **44** (1981) 709.

[7]  V. I. Arnold, Mathematical methods of classical mechanics (Springer, Berlin, 1978) App. 7.

[8]  C. Cerjan and W. P. Reinhardt, J. Chem. Phys. **71** (1979) 1819.

[9]  J. M. Green, J. Math. Phys. **9** (1968) 760 ; **20** (1979) 1183.

[10] A. Narita, Reserch Reports of Akita Technical College **19** (1984) 83.

[11] D. W. Noid, M. L. Koszykowski and R. A. Marcus, Ann. Rev. Phys. Chem. **32** (1981) 267.

[12] G. Casati and J. Ford, Phys. Rev. **A12** (1975) 1702.

[13] R. H. G. Helleman, in : Fundamental Problems in Statistical Mechanics, Vol. 5, E. G. D. Cohen, ed., (North−Holland, Amsterdam, 1980) p. 165.

[14] M. V. Berry, in : Topics in Nonlinear Dynamics, S. Jorna, ed., Am. Inst. Phys. Conf. Proc. (A. I. P., New York, 1978) Vol. 46, p. 16.

[15] J. Ford, in : Fundamental Problems in Statistical mechanics, Vol. 3, ed. E. G. D. Cohen, (North-Holland, Amsterdam, 1975) p. 215.

[16] C. L. Siegel and J. K. Moser, Lectures on Celestial Mechanics (Springer, New York, 1971).

[17] G. H. Walker and J. Ford, Phys. Rev. **188** (1969) 416.

[18] M. Hénon, Quart. Appl. Math. **27** (1969) 291.

[19] M. Toda, J. Phys. Soc. Japan **22** (1967) 431 ; **23** (1967) 501.

[20] M. K. Ali and R. L. Somorjai, Progr. Theor. Phys. **68** (1982) 1854.

[21] M. Hé non and C. Heiles, Astron. J. **69** (1964) 73.